

Chapter 20

Synthesis of Silver Nanoparticle Arrays for SERS Based Sensing

C. D'Andrea, F. Neri, P. M. Ossi, N. Santo and S. Trusso

Abstract Recently, noble-metal nanoparticles (NMNPs) were introduced in the sensing discipline, and become one of the most efficient ways to enhance sensors sensitivity. It is known, in fact, that NMNPs possess peculiar optical properties. When NMNPs are illuminated by a laser beam with proper wavelength, the so-called localized surface plasmons, a collective oscillation of conduction electrons on NMNP surface, are excited. The effect is relevant, for example, in Surface Enhanced Raman Spectroscopy, where a significant enhancement of a localized electromagnetic field near NMNPs surface allows to detect species usually undetectable with normal Raman spectroscopy. Here we present a method for the growth of silver NP arrays with controlled morphology by means of the pulsed laser ablation technique performed in presence of a Ar atmosphere. The nanoparticles size and morphology can be tuned, respectively, by the Ar pressure and the laser pulse number. The SERS activity of nanoparticle arrays is investigated by Raman scattering of adsorbed rhodamine 6G (R6G) at different concentrations.

C. D'Andrea · F. Neri

Dipartimento di Fisica della Materia e Ingegneria Elettronica, Università degli Studi di Messina, Viale F. Stagno D'Alcontres 31, 98166, Messina, Italy

P. M. Ossi

Dipartimento di Energia & Centre for NanoEngineered, MAterials and Surfaces NEMAS Politecnico di Milano, Via Ponzio 34-3, 20133, Milan, Italy

N. Santo

Centro Interdipartimentale di Microscopia Avanzata, Università degli Studi di Milano, Via Celoria 26, 20133, Milan, Italy

S. Trusso (✉)

Istituto per i Processi Chimico-Fisici, IPCF-CNR, V.le F. Stagno d'Alcontres 37, 98158 Messina, Italy
e-mail: trusso@me.cnr.it

20.1 Introduction

Raman spectroscopy is a highly versatile physico-chemical technique that provides information on vibrational modes from chemical species of samples. On the other hand nanostructured materials exhibit properties that are radically different from bulk form [1]. These effects are evident in the interaction of light with matter, such as, for example, in the Raman scattering processes. One of this is the Surface Enhanced Raman Scattering. This effect is characterized by a significant enhancement of a localized electromagnetic field (EM) near noble-metal nanoparticles (NMNPs) surface. The phenomenon of SERS is related to an electromagnetic mechanism, describing the surface electron movement in the nanoparticles and a chemical mechanism caused by charge transfer between the substrate and the analyte molecules [2]. The EM mechanism provides the largest contribution to the enhancement and is linked by the surface plasmon resonance (SPR) of NMNPs. In fact, when NMNPs are illuminated by a laser beam with proper wavelength, the SPR, a collective oscillation of conduction electrons on NMNPs surface, are excited. If the excitation light is resonant with a plasmon, the metal nanoparticles will emit electromagnetic radiation coherent with the exciting field that increases the total field. This is a near-field effect that, typically, is extinguished in less than 20 nm, so, only the analyte molecules near the nanostructure produce appreciable signal. Moreover, the nanostructures not only enhances the incident laser field, but also the Raman scattered field, so it is possible to obtain enhancement factor of 9–10 orders of magnitude. Varying the shape and size of nanostructures is, also, possible to involve different plasmon frequencies and modes.

The enormous enhancement of SERS effect allows to detect species usually undetectable with normal Raman spectroscopy. In the last years, in fact, there is a considerable interest in SERS effect as an ultra sensitive technique of detection of biomolecules such as cancer genes, hemoglobin, glucose and virus [3–5]. The high signal-to-noise ratios permit, also, to obtain in vivo tumor targeting and detection.

In this work we present a method for the growth of silver nanoparticle arrays with controlled morphology by means of the pulsed laser ablation technique performed in presence of argon atmosphere. The nanoparticles size and morphology can be tuned, respectively by the Ar gas pressure and the laser pulses number. The SERS activity of the nanoparticle arrays is investigated by Raman scattering of adsorbed Rhodamine 6G (R6G) at different concentrations.

20.2 Experiment

Silver thin films were grown by means of pulsed laser ablation using a KrF excimer laser ($\lambda = 248$ nm, pulse width 25 ns). The laser pulse is focused onto a pure silver target, positioned inside a vacuum chamber on a rotating holder in

order to avoid craterization phenomena. The substrate holder is positioned in front of the target at a distance of 35 mm. Different substrates were used: c-Si for scanning electron microscopy (SEM), a-C covered copper grids for transmission electron microscopy (TEM) and 7059 Corning glass for Raman and UV-Vis absorption spectroscopy. The other relevant deposition parameters, the laser fluence and the substrate temperature, were kept fixed at 2.0 J cm^{-2} and room temperature (RT), respectively. SEM imaging was carried out using a Zeiss Supra 40 field ion scanning microscope while TEM images were acquired with Zeiss Leo 912AB microscope. In order to test the SERS activity of the samples they were soaked into rhodamine 6G (R6G) aqueous solutions at different concentration for 1 h and then rinsed with deionized water. Four different R6G concentrations were tested in the range between 0.1 mM and 50 nM. Raman characterization was performed using a HR-800 Jobin-Yvon micro-Raman apparatus, using the 632.8 nm line of a He-Ne laser as the exciting source. The laser power incident on the samples surface was kept low, about $100 \text{ }\mu\text{W}$, in order to avoid R6G degradation. Raman spectra were acquired using a $10\times$ microscope objective resulting in a probe area of about $3.2 \text{ }\mu\text{m}^2$, while integration times were varied between 1 s up to 240 s, depending on the signal to noise ratio. UV-Vis spectra were acquired using a Lambda 900 Perkin Elmer spectrophotometer.

20.3 Results and Discussion

In Fig. 20.1 are reported the SEM images of the surface of the samples grown at the Ar pressure of 10, 40 and 70 Pa while the number of laser shots was kept fixed at 15,000. The surfaces are characterized by the presence of silver nanoparticles whose size and shape depend on the adopted Ar pressure. For the samples grown at 10 Pa of Ar, the presence of large NPs ($d > 35 \text{ nm}$), surrounded by a depletion area with smaller NPs, can be observed. On the other hand, for the samples deposited at 40 and 70 Pa of Ar (Fig. 20.1b, c) the surface is characterized by the presence of nearly spherical NPs with typical dimensions of 10 nm at 40 Pa and 5 nm at 70 Pa.

In previous works [6, 7] we studied the growth mechanism of silver thin films under deposition conditions similar to the ones adopted in this study. In particular our experiments gave evidence for a two step mechanism of film formation: in the first step the presence of the Ar atmosphere induces the aggregation between the silver atoms during the plasma expansion, leading to the formation of NPs; in the second step NPs landing on the substrates and having very low kinetic energies start to aggregate giving rise to larger NPs and finally to a coalesced structure characterized by the presence of an interconnected network of silver island with smooth rounded edges. The dimensions of the NPs, which form in flight, are determined by the Ar pressure [8]. The laser shot number, on the other side, drives the aggregation process on the substrates (at a fixed Ar pressure). By increasing the laser shots number the NP number density on the surface increases and NPs start to

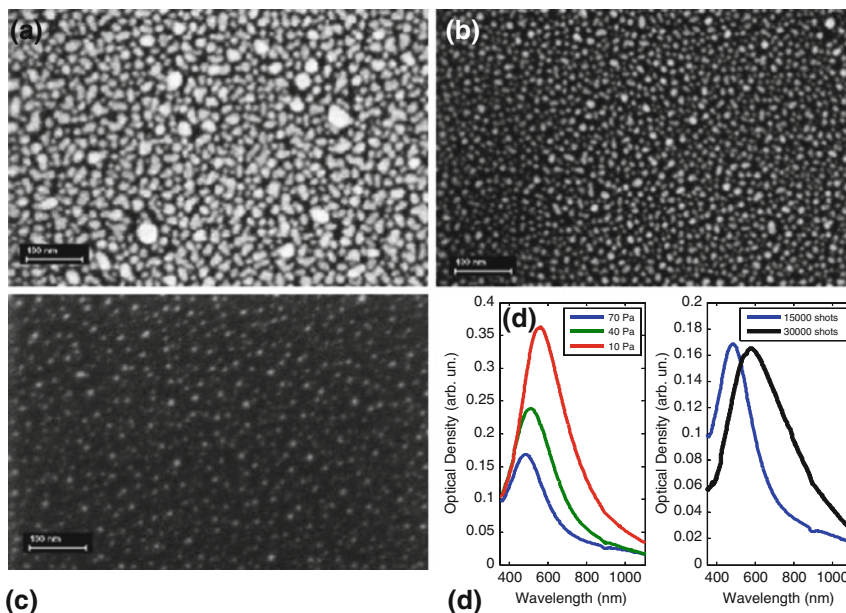
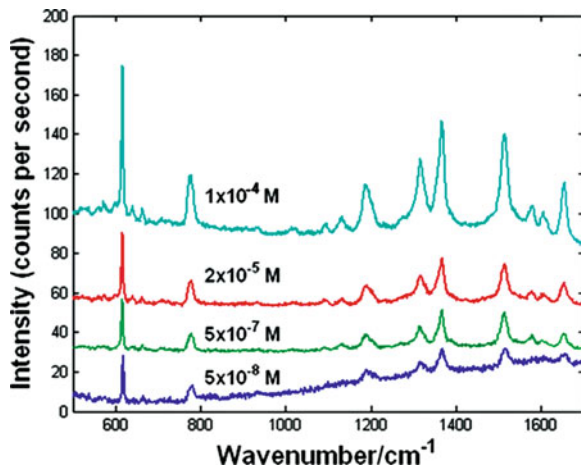


Fig. 20.1 SEM picture of the surface of the samples grown in Ar at **a** 10 Pa, **b** 40 Pa, **c** 70 Pa, using 15,000 laser shots. **d** Absorption spectra of the samples deposited at different Ar pressure and with different laser shots

aggregate. The different observed morphologies lead to different optical properties. Bulk silver shows an absorption peak in the near-UV, due to the coherent oscillations of surface electrons interacting with an external electromagnetic radiation, called surface plasmon resonance (SPR). When typical sizes are reduced to the nanoscale range, the SPR peak shifts to the visible region of the spectrum at about 390 nm. The position and shape of the SPR peak depend on size, shape and mutual aggregation properties of the nanostructures. In Fig. 20.1d are shown the UV–Vis absorption spectra of the samples deposited at different pressures. It can be observed that keeping fixed the number of laser shots at 15,000 and decreasing p_{Ar} from 70 Pa down to 10 Pa, the surface plasmon (SP) position red-shifts from 482 to 588 nm while its width progressively increases from 280 nm to more than 350 nm. A different behavior is observed for the plasmon position of the samples deposited at a fixed Ar pressure of 70 Pa.

The plasmon position red-shifts from 482 to 588 nm when the number of laser shots increases from 15,000 to 30,000. A larger broadening of the absorption band is evident for the sample grown at 30,000 pulses, highlighting that the film, deposited at the highest pulses number, consists of clustered NPs as observed from SEM images. A tuning of the plasmon position is then possible through both the laser pulses number and an appropriate Ar gas pressure. The SERS activity of the deposited film was tested soaking the samples for 1 h in rhodamine 6G (R6G)

Fig. 20.2 Raman spectra of the sample deposited at 70 Pa of Ar with 30,000 laser shots at different concentration of R6G



diluted aqueous solution with different concentration (1×10^{-4} , 2×10^{-6} , 5×10^{-7} and 5×10^{-8} M), rinsed with deionized water and dried in air.

In Fig. 20.2 are reported the Raman spectra of the sample deposited at 70 Pa of Ar with 30,000 laser shots at different concentration of R6G. The spectra are normalized to their own integration times. R6G dye Raman features can be observed at 615, 777, 1189, 1314, 1366, 1513 and $1,651 \text{ cm}^{-1}$ in the spectrum.

20.3.1 SERS Enhancement Factor

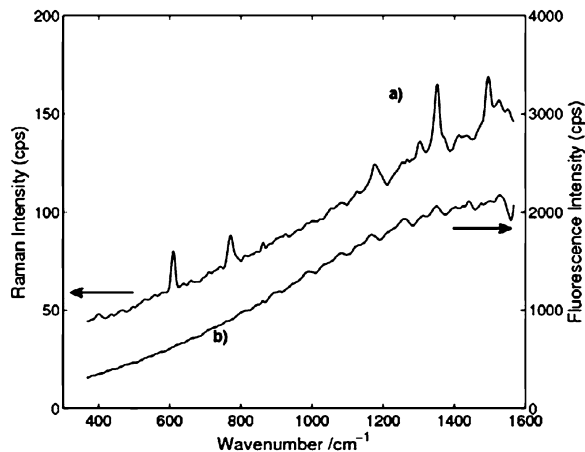
The quality of a SERS substrate can be evaluated by an estimate of the Raman enhancement factor (EF), defined as the ratio between the observed SERS intensity per molecule I_{SERS} and the normal Raman intensity per molecule I_{R} :

$$\text{EF} = \frac{I_{\text{SERS}}}{I_{\text{R}}} \frac{N_{\text{R}}}{N_{\text{SERS}}} \quad (20.1)$$

where N_{R} and N_{SERS} are the number of molecules which contribute to the normal Raman and the SERS intensities, respectively.

The Raman scattering cross section of R6G is of the order of 10^{-30} cm^{-2} and, since we were unable to detect any Raman signature in the spectra acquired on bare substrates soaked in the highest R6G aqueous solution, we evaluated the EF by comparing the Raman and the fluorescence intensities, according to the method described in [9]. In Fig. 20.3 is reported the Raman spectrum from a glass substrate covered with Ag NPs deposited in presence of 70 Pa of Ar and with 30,000 laser shots, soaked in the 1×10^{-4} M R6G solution, together with the spectrum acquired in the same experimental conditions but recorded on a bare glass substrate. The spectrum recorded from the bare substrate shows only the fluorescence contribution, while the other spectrum is characterized by the R6G features.

Fig. 20.3 Raman spectra of R6G adsorbed (a) on a glass substrate covered with silver nanoparticles (70 Pa of Ar, 30,000 shots) and (b) on a bare substrate (R6G concentration 1×10^{-4} M)



The difference between the fluorescence intensity recorded in the two spectra is about an order of magnitude and is probably due to fluorescence quenching following the energy transfer from the excited electronic state to the metal surface. Thus, I_R can be now evaluated using the relationship between the Raman intensity and the fluorescence signal. The Raman and the fluorescence cross sections at 514.5 nm, i.e., in resonant condition, are 10^{-25} and 10^{-16} cm^2 , respectively, so a factor of about 10^{-9} should be expected from the comparison of the two intensities. From Fig. 20.3 the intensity of the Raman peak at $1,360 \text{ cm}^{-1}$ is about 38 cps while the corresponding fluorescence signal is 1,978 cps. Thus the Raman scattering cross section is about two orders of magnitude lower than the fluorescence cross section resulting in an EF of the order of 10^7 .

20.4 Conclusions

We prepared, by pulsed laser ablation in presence of Ar gas, SERS active substrates suitable to detect the presence of R6G at concentrations as low as 5×10^{-8} M. Different surface morphologies, SP positions and hence SERS activities were obtained by controlling the laser pulses number and Ar gas pressure, keeping fixed all the other process parameters. The SERS enhancement factor was calculated to be about 10^7 .

References

1. Kelly KL, Jensen TA, Lazarides AA, Schatz GC (2002) Modeling metal nanoparticle optical properties. In: Feldheim DL, Foss CA Jr (eds) Metal nanoparticles: synthesis, characterization and applications. Dekker, New York, p 89
2. Banholzer MJ, Millstone JE, Qin L, Mirkin CA (2007) Rationally designed nanostructures for surface-enhanced Raman spectroscopy. Chem Soc Rev 37:885–897

3. Qian XM, Nie SM (2007) Single-molecule and single-nanoparticle SERS: from fundamental mechanisms to biomedical applications. *Chem Soc Rev* 37:912–920
4. Jarvis RM, Goodacre R (2007) Characterization and identification of bacteria using SERS. *Chem Soc Rev* 37:931–936
5. Murgida DH, Hildebrandt P (2007) Disentangling interfacial redox processes of proteins by SERR spectroscopy. *Chem Soc Rev* 37:937–945
6. Fazio E, Neri F, Ossi PM, Santo N, Trusso S (2009) Ag nanocluster synthesis by laser ablation in Ar atmosphere: a plume dynamics analysis. *Laser Particle Beams* 27:281–290
7. Fazio E, Neri F, Ossi PM, Santo N, Trusso S (2009) Growth process of nanostructured silver films pulsed laser ablated in high-pressure inert gas. *Appl Surface Sci* 255:9676–9679
8. Bailini A, Ossi PM (2007) Expansion of an ablation plume in a buffer gas and cluster growth. *Europhys Lett* 79:35002
9. Gupta R, Weimer WA (2003) High enhancement factor gold films for surface enhanced Raman spectroscopy. *Chem Phys Lett* 374:302–306